Matrix product simulations of non-equilibrium steady states of quantum spin chains

2009 J. Stat. Mech. 2009 P02035

(http://iopscience.iop.org/1742-5468/2009/02/P02035)

Journal of Statistical Mechanics: Theory and Experiment
An IOP and SISSA journal

Matrix product simulations of non-equilibrium steady states of quantum spin chains

Tomaž Prosen and Marko Žnidarič

Physics Department, Faculty of Mathematics and Physics,
University of Ljubljana, Jadranska 19, SI-1000 Ljubljana, Slovenia
E-mail: tomaz.prosen@fmf.uni-lj.si and marko.znidaric@fmf.uni-lj.si

Received 26 November 2008
Accepted 5 January 2009
Published 12 February 2009

Online at stacks.iop.org/JSTAT/2009/P02035
doi:10.1088/1742-5468/2009/02/P02035

Abstract. A time-dependent density matrix renormalization group method with a matrix product ansatz is employed for explicit computation of non-equilibrium steady state density operators of several integrable and non-integrable quantum spin chains, which are driven far from equilibrium by means of Markovian couplings to external baths at the two ends. It is argued that even though the time evolution cannot be simulated efficiently due to fast entanglement growth, the steady states in and out of equilibrium can be typically accurately approximated, with the result that chains of length of the order of $n \approx 100$ spins are accessible. Our results are demonstrated by performing explicit simulations of steady states and calculations of energy/spin densities/currents in several problems of heat and spin transport in quantum spin chains. A previously conjectured relation between quantum chaos and normal transport is re-confirmed with high accuracy for much larger systems.

Keywords: quantum chaos, entanglement in extended quantum systems (theory), quantum transport in one dimension, quantum transport

J. Stat. Mech. (2009) P02035

1742-5468/09/P02035+19$30.00

Contents

1. Introduction

A detailed understanding of the properties of strongly interacting many-particle quantum systems represents one of the major challenges of theoretical physics. Even for one spatial dimension (1D) and local interactions, very little is known about physics at high temperature, out of equilibrium, or for long real time evolution.

Quite recently, several original ideas emerging from the quantum information theory on the issue of entanglement in many-particle systems [1] resulted in very useful efficient techniques for the 'classical' simulation of quantum many-particle systems [2]. Even though most versions of these methods can be re-interpreted in terms of the *density matrix renormalization group* [3] (for an excellent review see [4]) and its time-dependent generalizations [5, 6] they bring in a conceptual simplification: namely, they represent the quantum many-body states in terms of the so-called finitely correlated states [7] which can be written in terms of matrix products, the so-called *matrix product states* (MPS). Similarly, the *matrix product operator* (MPO) ansatz can be used to describe density operators of mixed states [8, 9]. These ideas have been further developed by treating periodic boundary conditions [10], two-dimensional and higher lattices [11], translationally invariant systems [12, 13], and generalizing the MPS ansatz to tensor tree networks describing critical models [14]. For an extensive review, see [15].

However, most of these ingenious numerical methods turned out to be effective *only* for calculation of the ground states, low temperature equilibrium states, or time evolved states for short time or starting from particular (e.g. few-'quasi-particle', or locally excited) initial conditions (see e.g. [16]). The calculation of asymptotic time evolution in the thermodynamic limit, and the properties of *non-equilibrium steady states*

J. Stat. Mech. (2009) P02035

(NESS), remains notoriously difficult due to typical growth of bipartite entanglement in generic non-integrable systems and consequent exponential growth of the dimension of the relevant many-particle Hilbert space [17]. Therefore, the regularity to quantum chaos transition is manifested in the difficulty of classical simulation of quantum many-body dynamics [17]; see also [18]. Even though promising analytical techniques based on Fock spaces of operators have been developed recently in terms of which one can access NESS and relaxation properties of certain open integrable quantum many-body systems far from equilibrium [19, 20], for generic non-integrable systems one still needs to rely on more or less sophisticated 'brute force' methods limited at present to 20–30 1/2 spins (or qubits, fermions) in 1D. For such small systems it is often difficult or impossible to conclude on asymptotic thermodynamic properties due to considerable finite size effects.

In this paper we shall put forward a hypothesis that NESS of certain *open* 1D systems can be efficiently simulated in terms of the MPO ansatz.

Our idea is based on the following arguments. It has been shown rigorously that the ground states of several interacting many-particle systems in 1D can be written in terms of MPS (for example, the so-called *valence bond states* [21]). Later, it was shown [22]–[24], using the arguments of conformal field theory, that ground state entanglement entropy of a finite block of size n in any non-critical (gapped) system in 1D saturates with n, whereas for critical (non-gapped) systems the growth of the entanglement entropy is at most logarithmic in n. This result immediately implies that an efficient MPS representation of the ground states in 1D should exist, with the dimension of the parameterizing matrices saturating or growing not faster than polynomially with the system size n. A similar 'strong efficiency' result can be claimed for thermal states [25]. The defining equation for NESS of an open quantum system can be written as a 'right ground state' of a certain non-Hermitian quantum Liouville master operator [19]; hence NESS can be thought of as a kind of non-normal ground state in the Liouville space. This means that the entanglement of NESS, treated as an element of the Hilbert space of operators, can be relatively weak for a wide class of (non-integrable) problems even though the operator space entanglement of generic operators is much stronger (e.g. of the 'excited' eigenstates of Liouville master operator, i.e. decay modes). If this intuition is correct, then NESS should be simulated in terms of the MPO ansatz for systems considerably longer than 30 spins (at present).

In the present work we are going to test the MPO method on NESS calculation for different 1D systems, integrable and chaotic, as well as normal and ideal conductors. In particular, we shall focus on the problem of diffusive versus ballistic spin/heat transport in spin chains. There have been basically two approaches to quantum transport. The first one uses the linear response formalism, calculating equilibrium time correlation functions. In that approach one studies purely Hamiltonian systems, i.e., without any external baths, either directly (see e.g. [26]–[33]), or in terms of conformal field theory [34], or the quantum Monte Carlo method [35]. For exact calculations, spin chains of sizes up to $n = 28$ are achievable using a microcanonical finite temperature Lanczos method [31]. For a discussion of the applicability of the Green–Kubo formalism see [36]. The second approach proceeds via direct simulation of out-of-equilibrium system coupled to the baths, usually using a master equation [37]–[44], solving it by either numerical integration, diagonalization, or the Monte Carlo wavefunction approach. Using these methods one can study chains of up to $n = 20$ spins [41, 44].

doi:10.1088/1742-5468/2009/02/P02035

J. Stat. Mech. (2009) P02035

Using the MPO approach for solving the master equation proposed in the present paper we can calculate NESS of ∼100 spins. Even though we are at present unable to give a precise statement about the efficiency of the method for general NESS (for an exception due to exact solvability see [20]), the MPO approach should nevertheless prove very useful in studying out-of-equilibrium quantum many-body phenomena.

In section 2 we outline our numerical algorithm of computation of NESS in terms of the MPO ansatz as a time-asymptotic solution of the quantum (Lindblad) master equation. We also describe in detail efficient models of the baths used in our calculations. In sections 3 and 4 we discuss our numerical results for NESS and their transport properties in several integrable and non-integrable models of quantum spin chains, whereas in section 5 we summarize our findings and conclude.

2. The master equation

The most general completely positive trace preserving flow can be written in the form of a Lindblad equation [45] (see [46] for a comprehensive review on completely positive flows):

$$\frac{\mathrm{d}}{\mathrm{d}t}\rho = \mathrm{i}[\rho, H] + \gamma \sum_k ([L_k\rho, L_k^\dagger] + [L_k, \rho L_k^\dagger]) \tag{1}$$

(setting $\hbar = 1$) where H is the Hamiltonian, generating the unitary part of the evolution, L_k are Lindblad operators, and γ is some overall bath-coupling strength parameter. Formally, the solution of the linear Lindblad equation can be written as $\rho(t) = \exp(\hat{\mathcal{L}}t)\rho(0)$, where $\hat{\mathcal{L}}$ is a Liouvillian super-operator corresponding to the right-hand side of the Lindblad equation (1).

2.1. Matrix product operators and simulation of time evolution

We are going to simulate the time evolution under the Lindblad equation by using the MPO formulation. For a chain of n 1/2 spins, the density matrix ρ can always be expanded over all possible products of local Pauli operators which form a basis of the 4^n-dimensional Hilbert space of operators,

$$|\rho\rangle = \sum_{\underline{s}} c_{\underline{s}} |\sigma^{\underline{s}}\rangle, \tag{2}$$

where we use the shortened notation $\sigma^{\underline{s}} = \sigma_1^{s_1} \cdots \sigma_n^{s_n}$, $\underline{s} \equiv s_1, \ldots, s_n$, and $s_i \in \{0, 1, 2, 3\}$, with $\sigma^0 = \mathbb{1}, \sigma^1 = \sigma^x, \sigma^2 = \sigma^y, \sigma^3 = \sigma^z$. A lower index in the Pauli operators, for instance l in σ_l^s, will always denote a position $l \in \{1, \ldots, n\}$ of the spin on which it operates. In the MPO ansatz, the expansion coefficients $c_{\underline{s}}$ are represented in terms of $4n$ $D \times D$ matrices $\mathbf{A}_i^{s_i}$, $i = 1, \ldots, n$, as

$$c_{\underline{s}} = \mathrm{tr}\,(\mathbf{A}_1^{s_1} \cdots \mathbf{A}_n^{s_n}). \tag{3}$$

The propagator $\exp(\hat{\mathcal{L}}t)$ is implemented within the MPO formalism in small time steps of length τ (in our simulations $\tau = 0.05$). We decompose the Liouvillian as $\hat{\mathcal{L}} = \hat{\mathcal{L}}_1 + \hat{\mathcal{L}}_2$, with the condition that all the terms grouped within each $\hat{\mathcal{L}}_\nu$, $\nu = 1, 2$, mutually commute. For example, $\hat{\mathcal{L}}_1$ contains the terms with the interactions between the second and the

J. Stat. Mech. (2009) P02035

third spin, the fourth and the fifth spin, and so on, while $\hat{\mathcal{L}}_2$ contains the interactions between other pairs, whereas the corresponding one-body terms are distributed evenly between $\hat{\mathcal{L}}_1$ and $\hat{\mathcal{L}}_2$. For each small time step we use the Trotter–Suzuki formula, $\exp(\hat{\mathcal{L}}\tau) = \prod_k \exp(\alpha_k \hat{\mathcal{L}}_1 \tau) \exp(\beta_k \hat{\mathcal{L}}_2 \tau) + \mathcal{O}(\tau^p)$, with an appropriate scheme having either $p = 3$ or 4, depending on the required accuracy. The MPO representation of a density matrix ρ is exact only if the matrix dimension D of a matrix $\mathbf{A}_l^s$ at the lth site is equal to the number of non-zero Schmidt coefficients $\sqrt{\lambda_j}$ for a *bipartite* splitting of a super-ket $|\rho\rangle$ to the first l sites, denoted by A, and the remaining $n - l$ sites, denoted by B,

$$|\rho\rangle = \sum_j \sqrt{\lambda_j} |\xi_j^A\rangle |\xi_j^B\rangle, \tag{4}$$

with orthogonal vectors $|\xi_j^A\rangle$ and $|\xi_j^B\rangle$. Squares of the Schmidt coefficients, λ_j, ordered as $\lambda_1 \geq \lambda_2 \geq \cdots \geq 0$, are nothing but the eigenvalues of the reduced density matrix. The inner product is defined by $\langle \alpha | \beta \rangle = \mathrm{tr}\,(\alpha^\dagger \beta)/2^n$. Since the maximal number of non-zero Schmidt coefficients is usually exponentially large in n, one truncates the exact representation by keeping only a small fraction of largest $\sqrt{\lambda_j}$. An error made in such a truncation is given by a sum of truncated λ_j [47]. As a rough estimate of a minimal needed matrix dimension D one can use the Von Neumann entropy of a super-ket defined as $S^\sharp = -\sum_j \lambda_j \log_2 \lambda_j$, also called the *operator space entanglement entropy* (OSEE) (for an earlier definition in a different context see [48]). In terms of the coefficients $c_{\underline{s}}$, OSEE can be expressed as

$$S^\sharp = -\,\mathrm{tr}_A(\mathbf{R} \log_2 \mathbf{R}), \qquad \mathbf{R} = \langle \rho | \rho \rangle^{-1}\, \mathrm{tr}_B |\rho\rangle\langle\rho|, \tag{5}$$

where, again, a subscript A denotes the first l sites and B its complement. Writing the expansion coefficients $c_{\underline{s}}$ as a $2^l \times 2^{n-l}$-dimensional matrix $\mathbf{C}_{\underline{s}_A, \underline{s}_B} = c_{\underline{s}_A \underline{s}_B}$, the matrix $\mathbf{R}$ (5) is given by $\mathbf{R} = \mathbf{C}\mathbf{C}^{\mathrm{T}} / \mathrm{tr}\,(\mathbf{C}\mathbf{C}^{\mathrm{T}})$. OSEE is a measure of an entanglement of a super-ket $|\rho\rangle$ which, however, is a quantity essentially different from the entanglement of a mixed state represented by the density operator ρ. Also, OSEE is different from the ordinary von Neumann entropy of ρ. For instance, OSEE either saturates or grows logarithmically with time in an integrable transverse Ising model [49] or in the Heisenberg XXZ model in a random magnetic field [50], it saturates or grows linearly with n in NESS of an open XY spin chain [20], and it saturates or grows logarithmically with the inverse temperature for generic thermal states [25].

2.2. Physics and implementation of the baths

Let us say a few words about the details of our implementation of Markovian baths, that is of a non-unitary part $\hat{\mathcal{L}}_{\mathrm{B}}$ of $\hat{\mathcal{L}}$, involving Lindblad operators L_k, $\hat{\mathcal{L}}_{\mathrm{B}}\rho = \gamma \sum_k ([L_k \rho, L_k^\dagger] + [L_k, \rho L_k^\dagger])$. In our case—as our goal is to simulate *many-body coherent transport* in one dimension—the baths, i.e., the Lindblad operators L_k, will act only at the two *ends* of a 1D chain. More precisely, they will act just on the first and the last spin for a *single-spin* bath, or just on the first two and the last two spins for a *two-spin* bath. For a single-spin bath, we put $\hat{\mathcal{L}}_{\mathrm{B}}$ as part of $\hat{\mathcal{L}}_1$ as it commutes with all the other terms, so in the corresponding Suzuki–Trotter propagator, $\exp(\hat{\mathcal{L}}_{\mathrm{B}}\tau)$ factorizes out. Our choice of L_k will be such that $\hat{\mathcal{L}}_{\mathrm{B}}$ will have a single non-degenerate eigenvalue equal to 0 with the corresponding eigenvector ρ_B being a local equilibrium state, i.e. a direct product of

J. Stat. Mech. (2009) P02035

thermal states of (each of) the edge spins, or the pairs of the edge spins. Furthermore, due to the stability of completely positive dynamics, it is desirable for all other eigenvalues $\hat{\mathcal{L}}_{\rm B}$ to have negative real parts[1].

As a consequence, $\rho(t)$ will for sufficiently long time converge to NESS, $\rho_\infty = \lim_{t\to\infty} \exp(\hat{\mathcal{L}}t)\rho(0)$ of the entire spin chain, if we are starting from a generic initial state $\rho(0)$ having a non-zero overlap with ρ_∞. Due to the *ergodicity of the internal coherent dynamics* generated by the Hamiltonian H, we assume: (i) the resulting NESS ρ_∞ will be unique, i.e. independent of the details of the initial condition $\rho(0)$, (ii) the resulting NESS ρ_∞ will be (for *complex—say non-integrable and quantum chaotic—internal dynamics*) independent of the details of the bath operators L_k—and will only depend on thermodynamic bath parameters, such as temperature, magnetization, chemical potential, etc. Both assumptions have been carefully checked and confirmed in the numerical simulations which are reported below.

Note that the non-unitary part of evolution $\hat{\mathcal{L}}_{\rm B}$ does not preserve the Schmidt decomposition structure of matrices $\mathbf{A}_i^{s_i}$. Nevertheless, for small time steps, this breaking of orthogonality of Schmidt vectors is small. Therefore, we 're-orthogonalize' the matrices $\mathbf{A}_i^{s_i}$ by applying local rotations, recovering the Schmidt decomposition [2, 13], only every few time steps. We note that [8] originally proposed the idea of using the MPO for time-dependent solutions of the Lindblad master equation; however it was implemented in a physically essentially different context of systems with bulk dissipation where each spin has been monitored by a Lindbladian bath (see also [51]). The fact that the operator space entanglement is rather small in such a situation is not surprising; neither is the fact that it cannot be used to describe coherent out-of-equilibrium many-body phenomena.

The goal of the present paper is to test the efficiency of the MPO simulation of NESS as given by the asymptotic $t \to \infty$ solution of the master equation driven only by the *boundary* Lindblad terms, for different (integrable and non-integrable) 1D spin chains, checking along the way their transport behavior—being for instance that of a normal (diffusive) conductor, or anomalous transport. One expects that quantum chaotic systems will display normal conduction [29, 39], that is, they will obey Fourier/Fick/Ohm's law in which the current j is proportional to the gradient of a driving field ε, say the local energy density/temperature (or spin density/magnetization, or particle density/chemical potential, etc),

$$j = -\kappa \nabla \varepsilon. \tag{6}$$

For such normal conductors the transport properties should not depend on the details of the baths (assumption (ii) above). On the other hand, for the integrable models the choice of the baths could play a role. We are going to use two different models of the baths. In studies of the spin conduction in the Heisenberg model we will use a single-spin bath while we are going to use a two-spin bath when studying the energy transport in a quantum chaotic tilted Ising model. The reason for using a two-spin bath is the better (faster) convergence to NESS with time t and size n, which is probably due to the fact that the energy density is a two-body operator, while the spin density is a one-body operator.

[1] For an exact analysis of such open out-of-equilibrium quantum dynamics for Wigner–Jordan solvable models see [19, 20].

2.3. Single-spin bath

When studying the spin (magnetic) transport we are going to couple the first and the last spin of the chain to a single-spin bath. For simplicity we shall below write only one part of $\hat{\mathcal{L}}_{\rm B}$ pertaining to a given edge spin, with either $l = 1$ or n, and omitting the index l. In all our numerical simulations with the single-spin bath we shall take the coupling strength $\gamma = 1$.

There will be two Lindblad operators acting on the spin,

$$L_1 = \tfrac{1}{2}\sqrt{\Gamma_+}(\sigma^x + \mathrm{i}\,\sigma^y), \qquad L_2 = \tfrac{1}{2}\sqrt{\Gamma_-}(\sigma^x - \mathrm{i}\,\sigma^y), \qquad \Gamma_\pm = \sqrt{\frac{1 \mp \tanh\mu_{\rm L,R}}{1 \pm \tanh\mu_{\rm L,R}}}. \tag{7}$$

The stationary state for $\hat{\mathcal{L}}_{\rm B}$ constructed from the above operators is $\rho_{\rm B} = 1/(\Gamma_- + \Gamma_+)\mathrm{diag}(\Gamma_+, \Gamma_-) \propto \exp(-\mu_{\rm L,R}\sigma^z)$, with the average magnetization $\mathrm{tr}\,(\rho_{\rm B}\sigma^z) = -\tanh\mu_{\rm L,R}$. We stress that this is a stationary state of a single spin in the absence of Hamiltonian evolution. Parameters $\mu_{\rm L,R}$ of the left and the right bath, respectively, play the role of an external thermodynamic potential enforcing a spin density gradient, say a magnetization of a macroscopic magnet in contact with the edge spin. The matrix representation of a super-propagator $\exp(\hat{\mathcal{L}}_{\rm B}\tau)$ in the Pauli basis σ^α, $\alpha = 0, 1, 2, 3$, reads

$$\exp(\hat{\mathcal{L}}_{\rm B}\tau) = \begin{pmatrix} 1 & 0 & 0 & 0 \\ 0 & \mathrm{e}^{-(\Gamma_+ + \Gamma_-)\tau} & 0 & 0 \\ 0 & 0 & \mathrm{e}^{-(\Gamma_+ + \Gamma_-)\tau} & 0 \\ \frac{\Gamma_+ - \Gamma_-}{\Gamma_+ + \Gamma_-}\{1 - \mathrm{e}^{-2(\Gamma_+ + \Gamma_-)\tau}\} & 0 & 0 & \mathrm{e}^{-2(\Gamma_+ + \Gamma_-)\tau} \end{pmatrix}. \tag{8}$$

2.4. Two-spin bath

Here we would like to construct a bath $\hat{\mathcal{L}}_{\rm B}$, i.e. determine the corresponding Lindblad operators L_k, which produce a given unique stationary state $\rho_{\rm B}$ of a pair of spins, e.g. such that $\rho_{\rm B} = \exp(-h/T)/\,\mathrm{tr}\,\exp(-h/T)$ is a local thermal (Gibbs) state with respect to some two-spin energy density operator $h = h(\sigma_1^{s_1}, \sigma_2^{s_2})$. In all our numerical simulations with the two-spin bath we shall take the coupling strength $\gamma = 2$.

For the description of the methodology we shall assume that $\rho_{\rm B}$ is a known but completely general state given in terms of a 4×4 matrix. We require that $\rho_{\rm B}$ is a unique eigenvector of $\hat{\mathcal{L}}_{\rm B}$ with the corresponding eigenvalue 0, while all the other eigenvalues of $\hat{\mathcal{L}}_{\rm B}$ are negative. We are looking for a set of L_k such that the resulting $\hat{\mathcal{L}}_{\rm B}$ will have the above properties. With the constraints so far, the choice of the L_k is not unique, as we have fixed only one eigenvector and the corresponding eigenvalue of $\hat{\mathcal{L}}_{\rm B}$. So in addition we shall require that all other (negative) eigenvalues of $\hat{\mathcal{L}}_{\rm B}$ are equal to -1. Such $\hat{\mathcal{L}}_{\rm B}$ will produce the fastest possible convergence to $\rho_{\rm B}$ for a given fixed spectral norm of $\hat{\mathcal{L}}_{\rm B}$. Note that the eigenvalues of such optimized $\hat{\mathcal{L}}_{\rm B}$ do not necessarily imply maximal spectral gap of $\hat{\mathcal{L}}$ with a given bath-coupling strength, though we believe that this provides a good choice.

Assuming first that $\rho_{\rm B} = \mathrm{diag}(d_0, d_1, d_2, d_3)$ is diagonal one can easily check that the following set of Lindblad operators L_k:

$$L_{ij} = \sqrt{\frac{d_m}{32}}\, r^i \otimes r^j, \qquad i, j = 0, 1, 2, 3, \quad m = (i \bmod 2) + 2\,(j \bmod 2), \tag{9}$$

$$r^0 = \sigma^x + \mathrm{i}\,\sigma^y, \quad r^1 = \sigma^x - \mathrm{i}\,\sigma^y, \quad r^2 = \mathbb{I} + \sigma^z, \quad r^3 = \mathbb{I} - \sigma^z, \tag{10}$$

result in $\hat{\mathcal{L}}_{\mathrm{B}}^{\mathrm{diag}}$ satisfying the above conditions. Note that the above 16 Lindblad operators, labeled with a double index $k = (ij)$, can in fact be replaced by a set of 15 traceless operators leading to the same $\hat{\mathcal{L}}_{\mathrm{B}}^{\mathrm{diag}}$. In the Pauli basis the only non-zero matrix elements $(\mathcal{L}_{\mathrm{B}}^{\mathrm{diag}})_{\alpha,\beta}, \alpha, \beta \in \{0, \ldots, 15\}$ are (assuming positive d_i and $\mathrm{tr}\,\rho_{\mathrm{B}} = 1$)

$$\begin{aligned}
&(\hat{\mathcal{L}}_{\mathrm{B}}^{\mathrm{diag}})_{\alpha,\alpha} = -1, \qquad \alpha = 1, \ldots, 15,\\
&(\hat{\mathcal{L}}_{\mathrm{B}}^{\mathrm{diag}})_{15,0} = d_0 - d_1 - d_2 + d_3,\\
&(\hat{\mathcal{L}}_{\mathrm{B}}^{\mathrm{diag}})_{12,0} = d_0 + d_1 - d_2 - d_3,\\
&(\hat{\mathcal{L}}_{\mathrm{B}}^{\mathrm{diag}})_{3,0} = d_0 - d_1 + d_2 - d_3.
\end{aligned} \tag{11}$$

Basis states are enumerated in such a way that the least significant bit is the first one, i.e. corresponding to the left factor in the tensor products (9). Then, to obtain the bath operators L_k and $\hat{\mathcal{L}}_{\mathrm{B}}$ for a non-diagonal ρ_{B} we write the eigenvalue decomposition of $\rho_{\mathrm{B}} = V^\dagger d\, V$, where d is diagonal and V is unitary. In terms of the diagonal part d we first obtain the Lindblad super-operator $\hat{\mathcal{L}}_{\mathrm{B}}^{\mathrm{diag}}$ as described above in (9) and (11) and then rotate it in the operator space using the transformation R induced by V. Writing the orthogonal matrix of R in the Pauli basis $\sigma^{\underline{\alpha}} = \sigma^{\alpha_1} \otimes \sigma^{\alpha_2}$ we have $R_{\underline{\alpha},\underline{\beta}} = \mathrm{tr}\,(V^\dagger \sigma^{\underline{\beta}} V \sigma^{\underline{\alpha}})/4$, giving the final Lindblad propagator

$$\exp\,(\hat{\mathcal{L}}_{\mathrm{B}}\,\tau) = R^{\mathrm{T}} \exp\,(\hat{\mathcal{L}}_{\mathrm{B}}^{\mathrm{diag}}\,\tau) R. \tag{12}$$

3. Spin transport

Here we are going to study the spin transport in the Heisenberg XXZ model with the Hamiltonian

$$H = \sum_{l=1}^{n-1} (\sigma_l^x \sigma_{l+1}^x + \sigma_l^y \sigma_{l+1}^y + \Delta \sigma_l^z \sigma_{l+1}^z) + \sum_{l=1}^{n} h_l \sigma_l^z. \tag{13}$$

The first and the last spin will be coupled to a single-spin bath (8). The initial state is chosen to be a product state $\rho(t=0) \propto \exp\,(-\sum_l \mu_l \sigma_l^z)$, where μ_l linearly interpolates between the left/right bath values $\mu_{\mathrm{L,R}}$. We find that for times t of the order of several times n, the state practically converges to NESS ρ_∞, the properties of which we are interested in. In particular, in order to assess the validity of the spin Fick's law we are going to calculate the *magnetization profile* (also referred to as the spin profile), $S_l = \mathrm{tr}\,(\sigma_l^z \rho_\infty)$, and the local *spin current* defined as

$$j_l = \mathrm{tr}\,\big[(\sigma_l^x \sigma_{l+1}^y - \sigma_l^y \sigma_{l+1}^x)\rho_\infty\big]. \tag{14}$$

We are going to study three different parameter regimes of the Heisenberg model corresponding to the qualitatively different nature of many-body dynamics. The *integrable* XXZ Heisenberg model in the absence of magnetic field is known to display an ideal spin conduction for $\Delta < 1$ while it is probably a diffusive (normal) spin conductor for $\Delta > 1$ [27, 28, 30, 31]. The last statement is quite controversial in the light of the algebraic integrability of the model [52] so it will be inspected more carefully in the present paper. As the third case we shall study the spin transport in the XXZ model

J. Stat. Mech. (2009) P02035

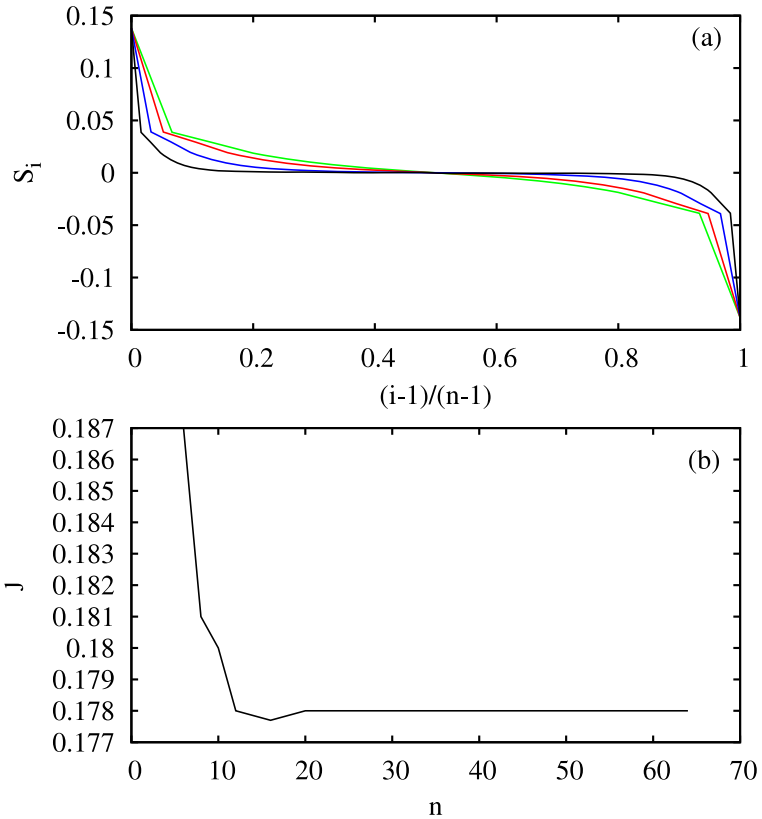

Figure 1. The spin profile (a) and the spin current (b) for the Heisenberg XXZ model at $\Delta = 0.5$ and bath couplings (7) with $\mu_{\mathrm{L,R}} = \pm 0.22$. Data for different chain lengths $n = 16, 20, 32, 64$, from green (bright) to black curves, are shown. With increasing n the spin profile gets flatter—an indication of an ideal spin conduction, visible also in the independence of the average spin current j on the chain length n in (b).

with a staggered transverse magnetic field in the regime of quantum chaos, significantly improving numerical evidence for the conjecture (put forward for the case of heat transport in [29, 39]) that quantum chaos corresponds to normal diffusive transport (Fourier's, Ohm's or Fick's law).

3.1. Ideally conducting regime, $\Delta = 0.5$

We will first take $\Delta = 0.5$ and no magnetic field, $h_l = 0$, in order to test the method in a regime where the Heisenberg model is an ideal spin conductor (having a non-vanishing Drude weight at any, say infinite temperature [28]). The left and the right bath parameters are set to $\mu_{\mathrm{L}} = 0.22$ and $\mu_{\mathrm{R}} = -0.22$. The results of numerical simulation are shown in figure 1. One can clearly see that the system is an ideal conductor, that is, it does not obey the spin Fick's law because the spin current is found to be proportional to the magnetization difference and *not* to its gradient. This is a typical property of completely integrable systems.

Considering the numerical efficiency of the MPO simulation of NESS, we show in figure 2 the Schmidt spectrum for a symmetric bipartite cut of NESS and different MPO

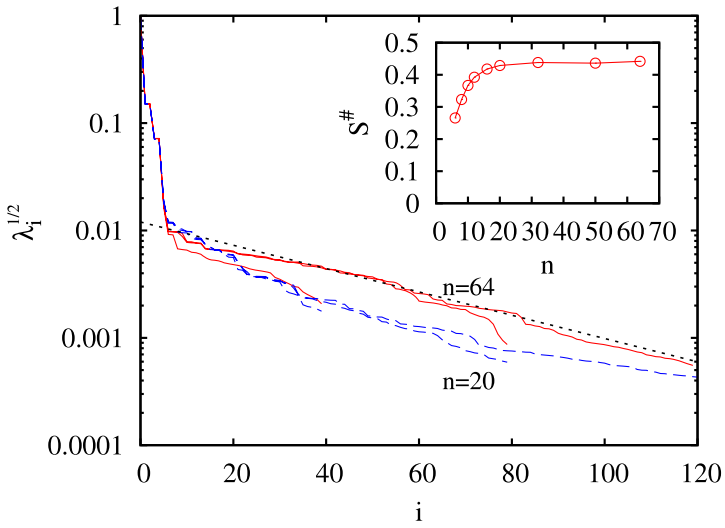

Figure 2. The spectrum of Schmidt coefficients $\sqrt{\lambda_i}$ for a symmetric bipartite splitting and different MPO dimensions $D = 40, 80, 120$ of the NESS in the Heisenberg model (13) with $\Delta = 0.5$ coupled to two single-spin baths with $\mu_{\mathrm{L,R}} = \pm 0.22$. Full (red) curves are for the chain size $n = 64$ while dashed (blue) curves are for $n = 20$. The dotted line indicates the exponential decay $\exp(-i/40)$. An inset shows the dependence of OSEE $S^\sharp$ (5) on n. $S^\sharp$ does not grow appreciably with n, indicating the efficiency of the MPO representation of NESS.

dimensions D. Numerical data suggest that the tails of the spectra of Schmidt coefficients decay *exponentially*. However, as these data are not very robust against changing n or D, we cannot exclude the possibility of other asymptotic decays. OSEE $S^\sharp$ (5) does not seem to grow with n (although on the basis of the numerics we cannot exclude a very slow growth) suggesting that the method is efficient, i.e. the computation time is asymptotically polynomial in n (linear in n if $S^\sharp(n)$ converges).

3.2. Normal conductor, $\Delta = 1.5$

On increasing Δ above 1 the Heisenberg model becomes a normal (diffusive) spin conductor (but *not* a diffusive heat conductor!) despite its integrability. We take $\Delta = 1.5$ in the absence of the magnetic field, $h_l = 0$, and a single-spin bath with a weak driving $\mu_{\mathrm{L,R}} = \pm 0.02$ (8) in order to make sure that non-linear transport features do not obscure the effect. Figure 3 clearly demonstrates that the system is indeed a normal spin conductor. The spin profiles in NESS are, apart from the boundary effects, perfectly linear. To reduce the boundary effects we drop the leftmost and the rightmost two spins when calculating the drop of the magnetization $\Delta S = S_{n-2} - S_3$, and its gradient $\nabla S = \Delta S/(n-4)$. The spin current is clearly proportional to the gradient of the magnetization ∇S, or for fixed bath data, to $\sim 1/n$; see figure 3(b). Note that the largest chain size $n = 100$ is much larger than what has been numerically achievable with other methods such as various Monte Carlo wavefunction approaches [39, 41, 42].

To show the convergence of $\rho(t)$ to the asymptotic NESS ρ_∞ we show in figure 4 the snapshots at different instants of time t of local spin current profiles j_i (14) and the

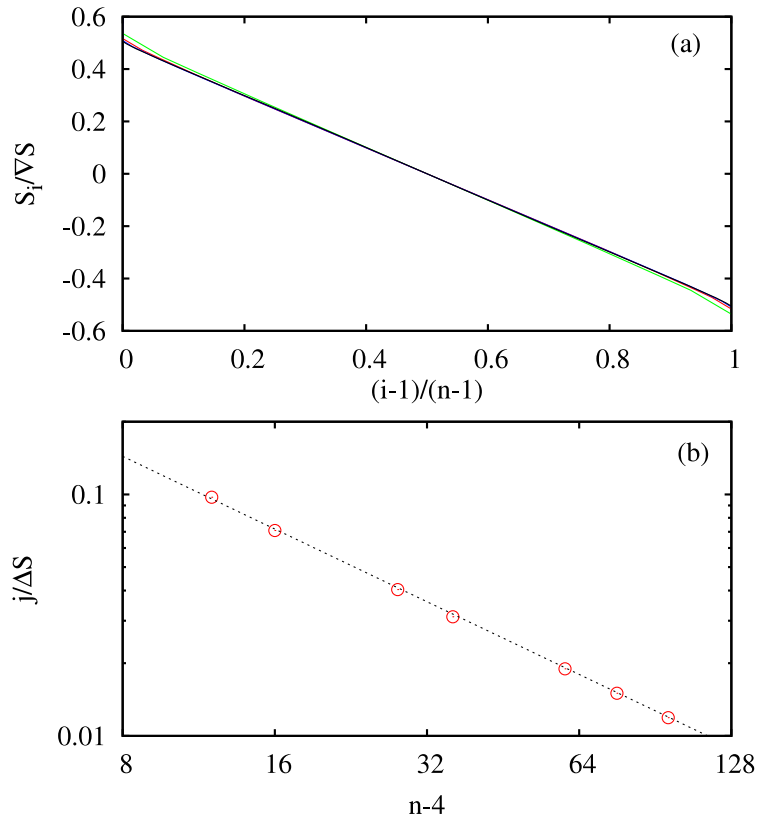

Figure 3. The spin profiles and the current versus system size in NESS for the Heisenberg XXZ model at $\Delta = 1.5$ and the bath-coupling parameters $\mu_{\mathrm{L,R}} = \pm 0.02$. Data for different chain lengths $n = 16, 32, 64, 100$, from green (bright) to black curves, almost overlap (frame (a)). Apart from the boundary effects the spin profile is linear, suggesting normal conduction and diffusive transport. This is confirmed in frame (b), where we show the dependence of the scaled spin current $j/\Delta S$ on the chain length n. The dotted line is $j/\Delta S \sim 1.15/(n-4)$, indicating spin 'Fick's law' with the spin conductivity $\kappa = 1.15$.

corresponding spectra of the Schmidt coefficients. Clearly, a tendency towards a uniform current profile for NESS required by the continuity equation is observed. Perhaps one would expect non-monotonic convergence of the Schmidt spectra, since for intermediate times $\rho(t)$ may be plagued by the decay modes which may be more complex to simulate than NESS. However, interestingly, in our simulations this typically does not happen, as shown in figure 4(b), and the effective Schmidt rank (or $S^\sharp$) typically *monotonically* converges with time t.

The tail of the Schmidt spectrum of NESS decays here (see figure 5 for our highest resolution data) qualitatively more slowly than for an ideally conducting case (e.g. $\Delta = 0.5$ of figure 2(b)), exhibiting perhaps an asymptotic power law decay, $\sqrt{\lambda_i} \sim 1/i^{1.25}$. Note that if the Schmidt coefficients decay algebraically as $\sqrt{\lambda_i} \sim 1/i^p$ with some power p, then the OSEE $S^\sharp$ converges to its exact value for $D \to \infty$ as $S^\sharp_{D=\infty} - S^\sharp_D \sim \log_2(D)/D^{2p-1}$. For our $p \approx 1.25$ this would mean a very slow $\sim \log_2(D)/D^{1.5}$ convergence of $S^\sharp$. Since

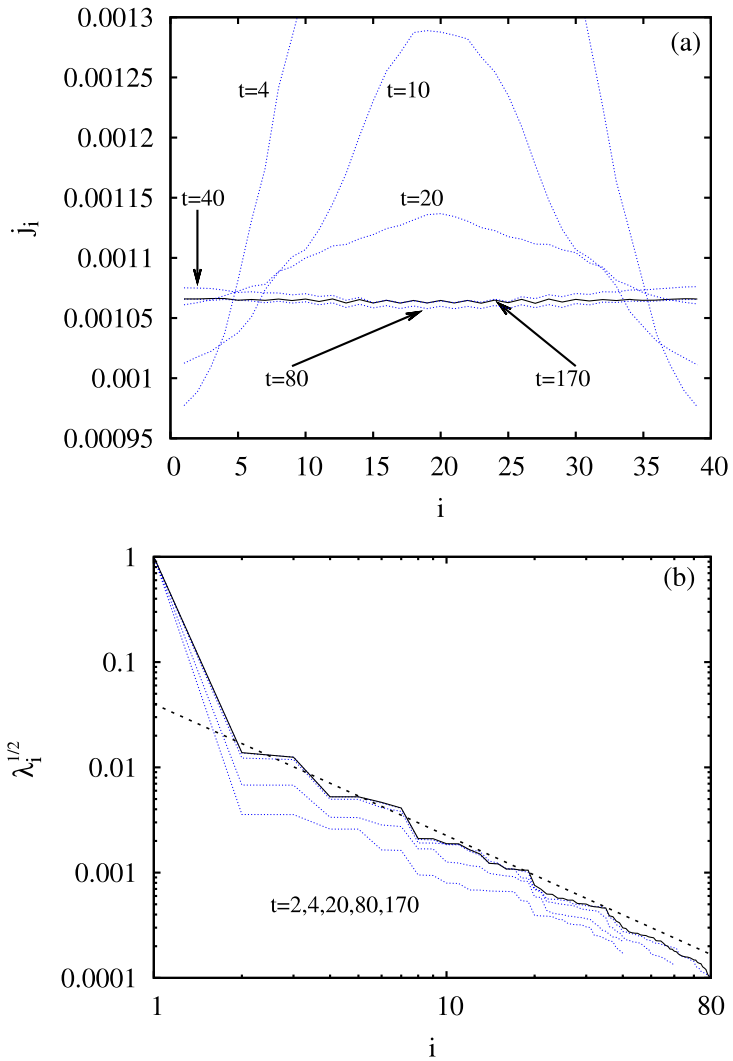

Figure 4. Convergence with time of the spin current profiles (dependence of the local current j_i on the lattice site i; frame (a)), and the convergence of the corresponding Schmidt spectra (frame (b)), for the Heisenberg XXZ model at $\Delta = 1.5$ (the case of figure 3) and for size $n = 40$. Snapshots at times as indicated in the figures are shown. We use $D = 40$ for $t = 2, 4, 10$, $D = 60$ for $t = 20$, and $D = 80$ for later times. Note that the Schmidt spectra converge much more quickly than the current profiles. The dotted line in (b) indicates a power law decay, $i^{-1.25}$.

we are limited to relatively small dimensions, of order $D \sim 100$, we are here not able to assess whether $S^\sharp$ saturates with n or not.

3.3. Normal conductor, $\Delta = 0.5$, and staggered transverse field

Here we are going to take the Heisenberg model (13) with $\Delta = 0.5$ and staggered transverse magnetic field, $h_{2l+1} = 0$ and $h_{2l} = -1/2$. We use the bath parameters $\mu_{\mathrm{L,R}} = \pm 0.1$. We have checked that for these parameter values the spectrum of the Hamiltonian (13)

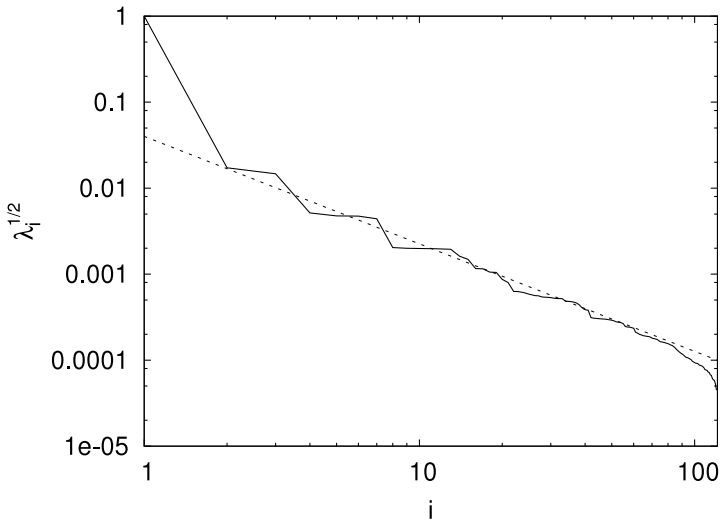

Figure 5. The spectrum of Schmidt coefficients $\sqrt{\lambda_i}$ of NESS (at convergence time $t = 250$) for a symmetric bipartite cut of the Heisenberg XXZ model at $\Delta = 1.5$. The MPO dimension is $D = 120$ and the spin chain length $n = 64$. The dotted line indicates a power law decay $i^{-1.25}$, with finite size effects setting in when $i \approx D$.

exhibits the characteristics of *quantum chaos*, i.e. the energy level spacing distribution agrees with universal predictions of random matrix theory with no free parameters, so the spin conduction is expected to be normally diffusive and to obey Fick's law. The results shown in figure 6 clearly confirm this expectation, namely the spin density profiles are linear, and the spin current decays as $\propto 1/n$. Note that this figure is very similar to figure 3 for the diffusive–integrable case with $\Delta = 1.5$; a subtle difference may be that now the boundary effects seem to be stronger. We have thus dropped border 5 spins at each end of a chain when calculating the spin drop $\Delta S = S_{n-5} - S_6$ and the gradient $\nabla S = \Delta S/(n - 10)$.

The tail of the Schmidt spectrum shown in figure 7 seems to decay even more slowly now, $\sqrt{\lambda_i} \sim 1/i^{0.80}$, making the simulation harder than in both integrable cases without the magnetic field. This is consistent with the previous observations in MPO simulations of long time evolution in the Heisenberg picture [17].

Useful information about the accuracy of NESS can also be obtained by computing the total truncation error per time step τ, for long times at the end of simulation. For example, for the case treated in figure 7, this truncation error is 3×10^{-4}, whereas in all other cases studied in this paper it has been smaller.

4. Energy transport

As the last test we are going to study the heat conductivity in the Ising model placed in a tilted magnetic field, the *tilted Ising model* for short, with the Hamiltonian

$$H = \sum_{l=1}^{n-1} h_{l,l+1}, \qquad h_{l,l+1} = -2\sigma_l^z \sigma_{l+1}^z + \tfrac{1}{2}(h_x \sigma_l^x + h_z \sigma_l^z) + \tfrac{1}{2}(h_x \sigma_{l+1}^x + h_z \sigma_{l+1}^z), \tag{15}$$

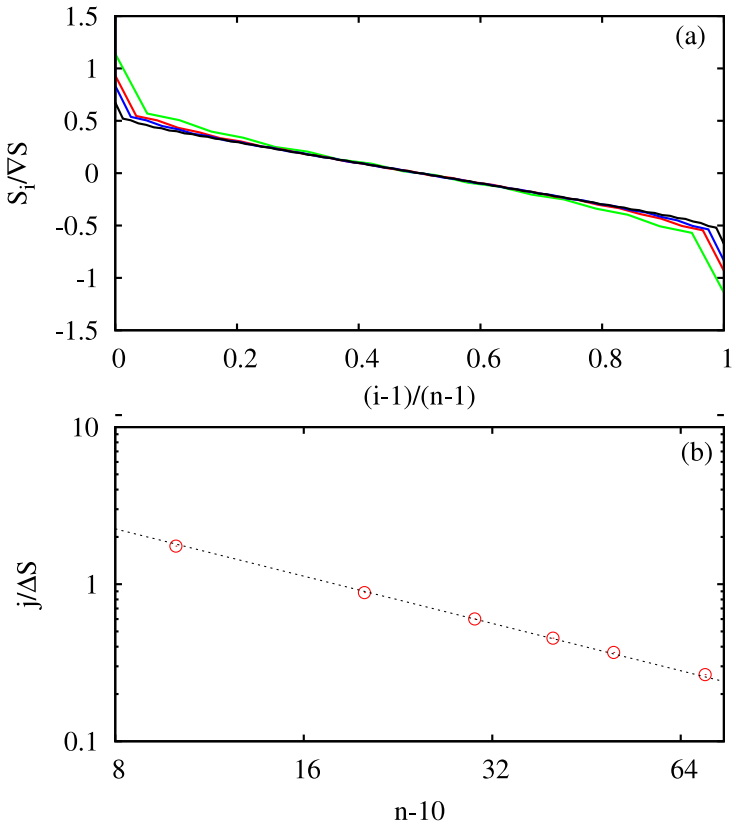

Figure 6. Spin profile (frame (a)) for the quantum chaotic Heisenberg XXZ model at $\Delta = 0.5$ in a staggered transverse field $h_l = (0, -0.5, 0, -0.5, \ldots)$. Data for chain lengths $n = 20, 30, 40, 80$, from green (bright) to black curves, are shown. Apart from the boundary effects the spin profile is linear, suggesting normal diffusive spin conduction. This is confirmed in frame (b), where we show the dependence of the scaled average spin current $j/\Delta S$ on n. The dotted line is $j/\Delta S \sim 18.0/(n-10)$, indicating 'Fick's law' with the spin conductivity $\kappa = 18.0$.

with $h_x = 3.375$ and $h_z = 2$. For these parameters the system is quantum chaotic (see e.g. [39]), and displays a normal heat conduction [39, 41]; however, previous simulations were limited to system sizes $n \leq 20$. For studies of heat transport in other quantum chaotic systems see also [29, 40]. The local energy current is in this case

$$j_l = 2h_x \,\mathrm{tr}\left[(\sigma_{l-1}^z \sigma_l^y - \sigma_l^y \sigma_{l+1}^z)\rho_\infty\right]. \tag{16}$$

When we used the single-spin bath (8) the convergence of the local energy current to a homogeneous site-independent value expected for NESS was rather slow, meaning that the spectral gap of the quantum Liouville operator $\hat{\mathcal{L}}$ is inconveniently small for such a bath model. Therefore, we rather used a two-spin bath (12) for which these effects are smaller. We set the temperature of the left bath to $T_\mathrm{L} = 20$ and of the right bath to $T_\mathrm{R} = 30$.

Since in an out-of-equilibrium system the definition of local temperature may not be completely unambiguous we have, instead of looking at the temperature profile, computed the energy density profile $\varepsilon_l = \mathrm{tr}\,\rho_\infty h_{l,l+1}$. As discussed in [39], the energy density

J. Stat. Mech. (2009) P02035

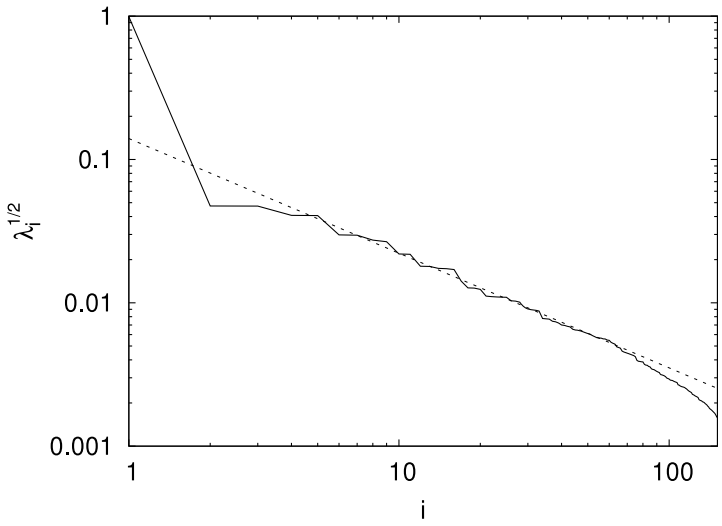

Figure 7. Spectrum of Schmidt coefficients $\sqrt{\lambda_i}$ of NESS (at convergence time $t = 200$) for a symmetric bipartite cut of the quantum chaotic Heisenberg model in a staggered field. The MPO dimension is $D = 150$ and size $n = 50$. The dotted line indicates a power law decay, $i^{-0.80}$.

uniquely determines the temperature in the equilibrium (thermal) state and it can also be used as a good measure of local temperature out of (but not too far from) equilibrium.

The boundary effects seen in figure 8 are again relatively strong. Because of these, and because we kept $T_{\mathrm{L,R}}$—which is a 'non-interacting temperature' of a two-spin system—fixed for all n, the actual local temperature varies slightly with n. In figure 8(a) we therefore appropriately shifted individual energy profiles in the vertical direction in order to obtain scaled overlapping curves. To decrease finite size effects at the boundaries we dropped border 4 spins when calculating the energy difference ΔE or the energy density gradient $\nabla E = \Delta E/(n-9)$ (figure 8).

Taking all of this into account, we have confirmed Fourier's law of heat conduction $j = \kappa \Delta E/(n-9)$, where ΔE was the energy density difference between $(5, 6)$ spins and $(n-5, n-4)$ spins, with an excellent numerical accuracy for $10 \leq n \leq 100$.

We have also looked (figure 9) at the tail of the spectrum of the Schmidt coefficients which is again consistent with a power law decay, namely the data are best fitted with $\sqrt{\lambda_i} \propto i^{-0.72}$.

5. Summary and discussion

In the present paper we have demonstrated numerical simulation of NESS for strongly but locally interacting open quantum systems in 1D in terms of the MPO ansatz. We have considered the most difficult case where the dynamics in the bulk is fully coherent (Hamiltonian), and dissipation (coupling to the baths) takes place only at the boundary (the ends of the chain). In this setting we have been able to confirm the laws of diffusive transport, such as Fourier's law of heat conduction and (the spin) Fick's law for spin conduction, in the cases where the underlying model is strongly non-integrable and displays the features of quantum chaos, or even when it is integrable but all the

doi:10.1088/1742-5468/2009/02/P02035

J. Stat. Mech. (2009) P02035

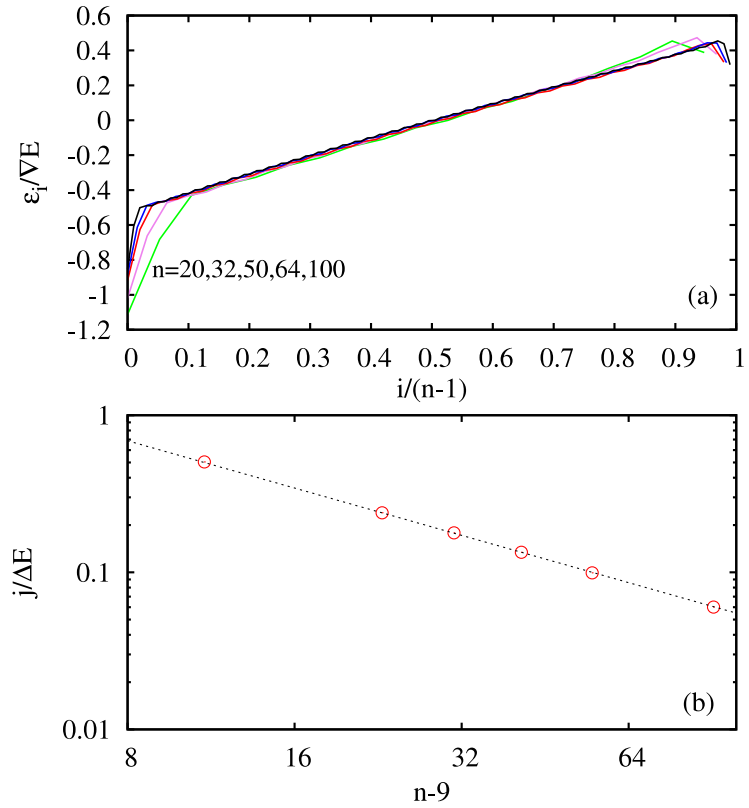

Figure 8. Local energy density profiles in NESS for the quantum chaotic tilted Ising model (15). Data for chain lengths $n = 20, 32, 50, 64, 100$, from green (bright) to black curves, almost overlap (frame (a)). Apart from the boundary effects the energy density profile is linear, suggesting normal heat conduction. This is confirmed in frame (b), where we show the dependence of the scaled energy current $j/\Delta E$ on n. The dotted line is $j/\Delta E \sim 5.5/(n-9)$, indicating the Fourier law behavior with the conductivity $\kappa = 5.5$.

conserved quantities are irrelevant for the transporting current, like in the case of spin conduction in the Ising-like Heisenberg XXZ chain. The main purpose of our paper was to demonstrate that such simulations were now possible for system sizes of order of $n = 100$ 1/2 spins, which is considerably larger than with the competing methods (usually based on Monte Carlo wavefunction techniques, where at present only $n \approx 20$ is reachable for fully out-of-equilibrium simulations).

As for the quantitative analysis of the efficiency of the MPO ansatz for NESS, we have analyzed the spectrum of the Schmidt decomposition for the worst-case (half–half) bipartition of the chain, when treating the density matrix of NESS as an element of the Hilbert space of operators. It is shown that the entanglement in such an operator space is clearly related to the efficiency of classical simulations of NESS.

Summarizing these results, we have found that *completely integrable* and *ideally conducting cases*, in our example the XY-like Heisenberg XXZ chain ($|\Delta| < 1$), are easiest to simulate since there the tail of the spectrum of Schmidt coefficients decays fastest, perhaps exponentially, so the MPO of a rather modest matrix dimension gives a good description of NESS.

doi:10.1088/1742-5468/2009/02/P02035

J. Stat. Mech. (2009) P02035

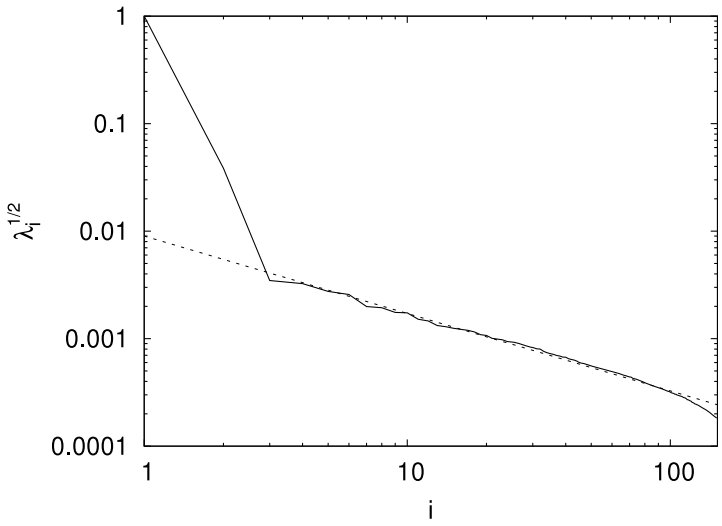

Figure 9. The spectrum of Schmidt coefficients $\sqrt{\lambda_i}$ of NESS (at convergence time $t = 500$) for a symmetric bipartite cut of the quantum chaotic tilted Ising model (for the case of figure 8). The MPO dimension is $D = 150$ and size $n = 50$. The dotted line indicates a power law decay, $i^{-0.72}$.

For still integrable systems, but for which all the conservation laws are irrelevant to the transporting current in NESS, such as the Ising-like Heisenberg XXZ chain ($|\Delta| > 1$), we have found qualitatively poorer efficiency, namely, there the tails of the Schmidt spectrum appear to exhibit power law tails $\sqrt{\lambda_i} \propto i^{-1.25}$.

Finally, for non-integrable systems in the regime of quantum chaos, the efficiency of simulation appears again poorer than in the integrable cases above (in our examples we have looked into the Heisenberg XXZ chain in a staggered transverse field, and the Ising spin chain in a tilted magnetic field). Namely, there we have found algebraically decaying tails of the Schmidt spectrum $\sqrt{\lambda_i} \propto i^{-p}$ with the power $p \in [0.7, 0.8]$.

On the basis of our results, we also conclude that zero-temperature (ground state) properties of the system, whether critical or gapped, do not influence far-from-equilibrium properties of NESS.

Acknowledgments

The work was financially supported by Program P1-0044 and Grant J1-7347 of the Slovenian Research Agency (ARRS).

References

[1] Amico L, Fazio R, Osterloh A and Vedral V, *Entanglement in many-body systems*, 2008 *Rev. Mod. Phys.* **80** 517
[2] Vidal G, *Efficient classical simulation of slightly entangled quantum computations*, 2003 *Phys. Rev. Lett.* **91** 147902
Vidal G, *Efficient simulation of one-dimensional quantum many-body systems*, 2004 *Phys. Rev. Lett.* **93** 040502
[3] White S R, *Density matrix formulation for quantum renormalization groups*, 1992 *Phys. Rev. Lett.* **69** 2863
[4] Schollwoeck U, *The density-matrix renormalization group*, 2005 *Rev. Mod. Phys.* **77** 259

J. Stat. Mech. (2009) P02035

[5] Daley A J, Kollath C, Schollwoeck U and Vidal G, *Time-dependent density-matrix renormalization-group using adaptive effective Hilbert spaces*, 2004 *J. Stat. Mech.* P04005

[6] Feiguin A E and White S R, *Real-time evolution using the density matrix renormalization group*, 2004 *Phys. Rev. Lett.* **93** 076401
Feiguin A E and White S R, *Finite-temperature density matrix renormalization using an enlarged Hilbert space*, 2005 *Phys. Rev.* B **72** 220401(R)

[7] Fannes M, Nachtergaele B and Werner R F, *Finitely correlated states on quantum spin chains*, 1992 *Commun. Math. Phys.* **144** 443

[8] Zwolak M and Vidal G, *Mixed-state dynamics in one-dimensional quantum lattice systems: a time-dependent superoperator renormalization algorithm*, 2004 *Phys. Rev. Lett.* **93** 207205

[9] Verstraete F, Garcia-Ripoll J J and Cirac J I, *Matrix product density operators: simulation of finite-temperature and dissipative systems*, 2004 *Phys. Rev. Lett.* **93** 207204

[10] Verstraete F, Porras D and Cirac J I, *Density matrix renormalization group and periodic boundary conditions: a quantum information perspective*, 2004 *Phys. Rev. Lett.* **93** 227205
Sandwik A W and Vidal G, *Variational quantum Monte Carlo simulations with tensor-network states*, 2007 *Phys. Rev. Lett.* **99** 220602
Pippan P, White S R and Evertz H G, *Improved scaling for periodic matrix product state algorithms*, 2008 arXiv:0801.1947

[11] Verstraete F and Cirac J I, *Renormalization algorithms for quantum-many body systems in two and higher dimensions*, 2004 arXiv:cond-mat/0407066

[12] Vidal G, *Classical simulation of infinite-size quantum lattice systems in one spatial dimension*, 2007 *Phys. Rev. Lett.* **98** 070201

[13] Orus R and Vidal G, *Infinite time-evolving block decimation algorithm beyond unitary evolution*, 2008 *Phys. Rev.* B **78** 155117

[14] Shi Y-Y, Duan L-M and Vidal G, *Classical simulation of quantum many-body systems with a tree tensor network*, 2006 *Phys. Rev.* A **74** 022320
Vidal G, *Entanglement renormalization*, 2007 *Phys. Rev. Lett.* **99** 220405

[15] Murg V, Verstraete F and Cirac J I, *Matrix product states, projected entangled pair states, and variational renormalization group methods for quantum spin systems*, 2009 *Rev. Mod. Phys.* at press

[16] Perales A and Vidal G, *Entanglement growth and simulation efficiency in one-dimensional quantum lattice systems*, 2008 *Phys. Rev.* A **78** 042337

[17] Prosen T and Žnidarič M, *Is the efficiency of classical simulations of quantum dynamics related to integrability?*, 2007 *Phys. Rev.* E **75** 015202

[18] Venzl H, Daley A J, Mintert F and Buchleitner A, *Simulability and regularity of complex quantum systems*, arXiv:0808.3911

[19] Prosen T, *Third quantization: a general method to solve master equations for quadratic open Fermi systems*, 2008 *New J. Phys.* **10** 043026

[20] Prosen T and Pižorn I, *Quantum phase transition in a far-from-equilibrium steady state of XY spin chain*, 2008 *Phys. Rev. Lett.* **101** 105701

[21] Affleck I, Kennedy T, Lieb E H and Tasaki H, *Valence bond ground states in isotropic quantum antiferromagnets*, 1988 *Commun. Math. Phys.* **115** 477

[22] Callan C and Wilczek F, *On geometric entropy*, 1994 *Phys. Lett.* B **333** 55

[23] Vidal G, Latorre J I, Rico E and Kitaev A, *Entanglement in quantum critical phenomena*, 2003 *Phys. Rev. Lett.* **90** 227902
Latorre J I, Rico E and Vidal G, *Ground state entanglement in quantum spin chains*, 2004 *Quantum Inf. Comput.* **4** 48

[24] Calabrese P and Cardy J, *Entanglement entropy and quantum field theory*, 2004 *J. Stat. Mech.* P06002

[25] Žnidarič M, Prosen T and Pižorn I, *Complexity of thermal states in quantum spin chains*, 2008 *Phys. Rev.* A **78** 022103

[26] Castella H, Zotos X and Prelovšek P, *Integrability and ideal conductance at finite temperatures*, 1995 *Phys. Rev. Lett.* **74** 972

[27] Narozhny B N, Millis A J and Andrei N, *Transport in the XXZ model*, 1998 *Phys. Rev.* B **58** R2921

[28] Zotos X, *Finite temperature Drude weight of the one-dimensional spin-1/2 Heisenberg model*, 1999 *Phys. Rev. Lett.* **82** 1764

[29] Saito K, *Strong evidence of normal heat conduction in a one-dimensional quantum system*, 2003 *Europhys. Lett.* **61** 34

[30] Heidrich-Meisner F, Honecker A, Cabra D C and Brenig W, *Zero-frequency transport properties of one-dimensional spin-1/2 systems*, 2003 *Phys. Rev.* B **68** 134436

J. Stat. Mech. (2009) P02035

[31] Long M W, Prelovšek P, El Shawish S, Karadamoglou J and Zotos X, *Finite-temperature dynamical correlations using the microcanonical ensemble and the Lanczos algorithm*, 2003 *Phys. Rev.* B **68** 235106
Prelovšek P, El Shawish S, Zotos X and Long M, *Anomalous scaling of conductivity in integrable fermion systems*, 2004 *Phys. Rev.* B **70** 205129
[32] Klümper A and Sakai K, *The thermal conductivity of the spin-XXZ chain at arbitrary temperature*, 2002 *J. Phys. A: Math. Gen.* **35** 2173
Sakai K and Klümper A, *Non-dissipative thermal transport in the massive regimes of the XXZ chain*, 2003 *J. Phys. A: Math. Gen.* **36** 11617
[33] Pereira R G, Sirker J, Caux J-S, Hagemans R, Maillet J M, White S R and Affleck I, *Dynamical spin structure factor for the anisotropic spin-1/2 Heisenberg chain*, 2006 *Phys. Rev. Lett.* **96** 257202
[34] Fujimoto S and Kawakami N, *Drude weight at finite temperatures for some nonintegrable quantum systems in one dimension*, 2003 *Phys. Rev. Lett.* **90** 197202
[35] Alvarez J V and Gros C, *Low-temperature transport in Heisenberg chains*, 2002 *Phys. Rev. Lett.* **88** 077203
[36] Gemmer J, Steinigeweg R and Michel M, *Limited validity of the Kubo formula for thermal conduction in modular quantum systems*, 2006 *Phys. Rev.* B **73** 104302
[37] Saito K and Miyashita S, *Enhancement of the thermal conductivity in gapped quantum spin chains*, 2002 *J. Phys. Soc. Japan* **71** 2485
[38] Michel M, Hartmann M, Gemmer J and Mahler G, *Fourier's law confirmed for a class of small quantum systems*, 2003 *Eur. Phys. J.* B **34** 325
[39] Mejia-Monasterio C, Prosen T and Casati G, *Fourier's law in a quantum spin chain and the onset of quantum chaos*, 2005 *Europhys. Lett.* **72** 520
[40] Steinigeweg R, Gemmer J and Michel M, *Normal-transport behavior in finite one-dimensional chaotic quantum systems*, 2006 *Europhys. Lett.* **75** 406
[41] Mejia-Monasterio C and Wichterich H, *Heat transport in quantum spin chains—stochastic baths versus quantum trajectories*, 2007 *Eur. Phys. J. Spec. Top.* **151** 113
[42] Wichterich H, Henrich M J, Breuer H-P, Gemmer J and Michel M, *Modeling heat transport through completely positive maps*, 2007 *Phys. Rev.* E **76** 031115
[43] Yan Y, Wu C-Q, Casati G, Prosen T and Li B, *Nonballistic heat conduction in an integrable random-exchange Ising chain studied with quantum master equations*, 2008 *Phys. Rev.* B **77** 172411
[44] Michel M, Hess O, Wichterich H and Gemmer J, *Transport in open spin chains: a Monte Carlo wavefunction approach*, 2008 *Phys. Rev.* B **77** 104303
[45] Lindblad G, *On the generators of quantum dynamical semigroups*, 1976 *Commun. Math. Phys.* **48** 119
[46] Alicki R and Lendi K, 2007 *Quantum Dynamical Semigroups and Applications* (Berlin: Springer)
[47] Schuch N, Wolf M M, Verstraete F and Cirac J I, *Entropy scaling and simulability by matrix product states*, 2008 *Phys. Rev. Lett.* **100** 030504
[48] Zanardi P, *Entanglement of quantum evolutions*, 2001 *Phys. Rev.* A **63** 040304(R)
Nielsen M A, Dawson C M, Dodd J L, Gilchrist A, Mortimer D, Osborne T J, Bremner M J, Harrow A W and Hines A, *Quantum dynamics as a physical resource*, 2003 *Phys. Rev.* A **67** 052301
[49] Prosen T and Pižorn I, *Operator space entanglement entropy in transverse Ising chain*, 2007 *Phys. Rev.* A **76** 032316
[50] Žnidarič M, Prosen T and Prelovšek P, *Many body localization in Heisenberg XXZ magnet in a random field*, 2008 *Phys. Rev.* B **77** 064426
[51] Hartmann M J and Plenio M B, *DMRG in the Heisenberg picture*, 2008 arXiv:0808.0666
[52] Zotos X, Naef F and Prelovšek P, *Transport and conservation laws*, 1997 *Phys. Rev.* B **55** 11029

J. Stat. Mech. (2009) P02035